MOLECULAR AND CELLULAR BIOLOGY, Apr. 1995, p. 1942–1952 Vol. 15, No. 4
0270-7306/95/$04.00+0

The Ras-Related Protein Cdc42Hs and Bradykinin Promote Formation of Peripheral Actin Microspikes and Filopodia in Swiss 3T3 Fibroblasts

ROBERT KOZMA,[1,2]* SOHAIL AHMED,[1,2] ANTHONY BEST,[1] AND LOUIS LIM[1,2]

Institute of Neurology, London WC1N 1PJ, United Kingdom,[1] and Institute of Molecular and Cell Biology, National University of Singapore, Singapore 0511, Singapore[2]

Received 27 October 1994/Returned for modification 7 December 1994/Accepted 30 December 1994

The Ras-related protein Cdc42 plays a role in yeast cell budding and polarity. Two related proteins, Rac1 and RhoA, promote formation in mammalian cells of membrane ruffles and stress fibers, respectively, which contain actin microfilaments. We now show that microinjection of the related human Cdc42Hs into Swiss 3T3 fibroblasts induced the formation of peripheral actin microspikes, determined by staining with phalloidin. A proportion of these microspikes was found to be components of filopodia, as analyzed by time-lapse phase-contrast microscopy. The formation of filopodia was also found to be promoted by Cdc42Hs microinjection. This was followed by activation of Rac1-mediated membrane ruffling. Treatment with bradykinin also promoted formation of microspikes and filopodia as well as subsequent effects similar to that seen upon Cdc42Hs microinjection. These effects of bradykinin were specifically inhibited by prior microinjection of dominant negative Cdc42Hs^{T17N}, suggesting that bradykinin acts by activating cellular Cdc42Hs. Since filopodia have been ascribed an important sensory function in fibroblasts and are required for guidance of neuronal growth cones, these results indicate that Cdc42Hs plays an important role in determining mammalian cell morphology.

The Ras-related Rho subfamily of low-molecular-weight GTP-binding proteins (p21s) are thought to play roles in cell polarity, migration, and division (21). In mammals, the Rho family is composed of a number of closely related (>50% sequence identity) proteins, which include Rac1 and -2, RhoA, -B and -C, and Cdc42Hs. These proteins are thought to cycle between GTP-bound (on) and GDP-bound (off) states. Proteins that regulate their cycling include GTPase-activating proteins (GAPs) such as the breakpoint cluster region gene product (Bcr) and *n*-chimerin (14) as well as GDP/GTP exchange factors such as Dbl (23). These regulators may also be target proteins involved in effector function (34).

The first indication that p21s may be involved in determining cell morphology came from experiments microinjecting Ras into mammalian cells, which resulted in membrane ruffling (6). Furthermore, addition of *Clostridium botulinum* C3 exoenzyme, which ADP ribosylates Rho specifically, causes cells to lose stress fibers and to round up (10, 39). The cellular functions of RhoA and Rac1 have been directly investigated by monitoring changes in the cellular actin cytoskeleton induced after microinjection of these proteins into Swiss 3T3 cells. RhoA and Rac1 promote the formation of the actin microfilament structures and of stress fibers and membrane ruffles, respectively (39–41). By using dominant negative mutant p21 proteins (T17N, where Thr-17 has been changed to Asn) which are specific inhibitors of endogenous p21 signalling pathways, it has been shown that platelet-derived growth factor (PDGF), phorbol myristate acetate (PMA), and Ras-GTP induce membrane ruffling by activating the Rac1 pathway. Rac1 can also activate the RhoA-mediated stress fiber formation (41) and the neutrophil oxidase (1, 29).

Cdc42 was originally detected in the yeast *Saccharomyces cerevisiae* as a mutation that caused defects in budding and cell polarity (2, 15, 27). Human Cdc42Hs can complement the yeast mutant (36, 43), but its function in mammalian cells is not known. We recently reported the characterization of potential cellular targets for mammalian Cdc42Hs, including the tyrosine kinase p120^{ACK} (32) and the serine/threonine kinase p65^{PAK} (33), which bind the p21 only in its GTP form. Their function remains to be established. The *dbl* oncogene is a GDP/GTP exchange factor and potential activator of Cdc42Hs, implying a role for Cdc42Hs in cell transformation (23). Here, we show that microinjection of Cdc42Hs into serum-starved, subconfluent Swiss 3T3 cells induced the formation of actin-containing microspikes at the cell periphery. Some of these peripheral actin microspikes (PAM) were found to be components of filopodia, as determined by time-lapse phase-contrast microscopy. Filopodia are actin-containing structures which have been proposed to have an important sensory function in Swiss 3T3 cells (5) and in neural growth cones (11, 26). The formation of filopodia promoted by Cdc42Hs microinjection, with accompanying cell retraction, was followed by membrane ruffling and lamellipodium formation. Actin staining of Cdc42Hs-microinjected cells also revealed a loss of stress fibers. Among a variety of growth factors examined, bradykinin was the only one found to mimic all of the effects of Cdc42Hs microinjection. The use of dominant negative proteins allowed us to determine the specificity of the responses elicited by bradykinin. Filopodium formation was inhibited by Cdc42Hs^{T17N}, while Rac1^{T17N} inhibited only ruffling and lamellipodium formation. These results suggest that Cdc42Hs plays an important role in determining mammalian cell shape and cell polarity, possibly by causing specific changes in actin polymerization.

* Corresponding author. Mailing address: Department of Neurochemistry, Institute of Neurology, 1 Wakefield St., London WC1N 1PJ, United Kingdom. Phone: 071-278-1552. Fax: 071-278-7045.

MATERIALS AND METHODS

Subcloning, site-directed mutagenesis, and protein expression. Rac1, RhoA, Cdc42Hs, and Rho-GDP dissociation inhibitor (GDI) cDNAs were subcloned into pGEX-2T (44) derivatives p265 (3) and p265polyG, derivatives of p265 with a polyglycine spacer between the thrombin cleavage site and cDNA cloning site (20). This latter vector generated fusion proteins that were better substrates for thrombin cleavage. Mutagenesis was carried out by using the Clontech Transformer Site-Directed Mutagenesis kit on cDNAs subcloned in pBluescript. Mutants were sequenced before subcloning into *Escherichia coli* expression vector p265 or p265polyG. The *n*-chimerin cDNA domain expression vector was as described previously (14). For protein purification, *E. coli* cells carrying an appropriate plasmid were grown to an optical density at 650 nm of 0.5, and isopropylthiogalactoside (1 mM) was added. Cells were harvested, resuspended in a mixture of thrombin cleavage buffer, phenylmethylsulfonyl fluoride (1 mM), and a cocktail of protease inhibitors and then frozen at −20°C. When required, cells were thawed and sonicated (four times for 30 s each, setting 4, MSE sonicator), and cell debris was removed by centrifugation at 14,000 × *g* for 10 to 20 min. Supernatants were then applied to glutathione-Sepharose columns, proteins were eluted with thrombin, and the thrombin was removed by using benzadiamine-Sepharose columns. Proteins were frozen (−20°C) in aliquots. All proteins were greater than 95% pure as determined by image analysis of proteins separated on sodium dodecyl sulfate-polyacrylamide gels, using a Quantimet 570 image analyzer (Cambridge Instruments). The GTPase activities of Cdc42Hs and Cdc42Hs mutants (G12V and Q61L) were measured as previously described (4). Over a 10-min time course at 15°C, the proportions of GTP hydrolyzed were 25% for wild-type Cdc42Hs, 5% for the G12V mutant, and 0% for the Q61L mutant.

Cell microinjection and staining. Swiss 3T3 cells were grown on ethanol-washed glass slides (gridded to allow relocation of microinjected cells) in Dulbecco's modified Eagle medium plus 10% fetal calf serum (FCS; Gibco) at 37°C in 5% CO_2. Subconfluent cells were starved in Dulbecco's modified Eagle medium plus 0.2% $NaHCO_3$ for 48 h before injection. Proteins were normally microinjected in 20 mM Tris-HCl (pH 7.4), using an Eppendorf microinjector and Zeiss Axiovert microscope. Successful injection was determined visually at time of injection or also by coinjection of a marker protein such as mouse immunoglobulin γ. Cell viability was estimated to be greater than 90%. For time-lapse studies, the cells were maintained on a heated platform (37°C) and viewed under phase contrast. For actin staining, the cells were incubated for the appropriate time before being washed with phosphate-buffered saline (PBS), fixed in 3% paraformaldehyde in PBS for 20 min, and washed in 0.2% Triton X-100 in PBS for 5 min. Slides were then stained with rhodamine-conjugated phalloidin (0.2 mg/ml; Sigma) (to stain filamentous actin) in PBS for 1 h, washed in PBS three times for 3 min each, briefly washed in water, and finally mounted in Mowiol–1,4-diazabicyclo(2.2.2) octane (DABCO) (Aldrich). Cells were photographed under fluorescence, using Ektachrome 400 film (Kodak), or under phase contrast, using PAN F 50 film (Ilford). Quantification was carried out from photographic records of the experiments.

Reagents. PMA, lysophosphatidic acid (LPA), bradykinin, bombesin, insulin, and 1-oleyl-2-acetyl-rac-glycerol were from Sigma, PDGF was from Amersham, and epidermal growth factor (EGF) was from Boehringer Mannheim.

RESULTS

Cdc42Hs induces the formation of PAM and ruffles. To investigate the function of Cdc42Hs, we microinjected serum-starved Swiss 3T3 cells with purified recombinant protein and monitored changes in actin-containing structures by staining with rhodamine-conjugated phalloidin. Within a few minutes of microinjection with Cdc42Hs, actin filaments were seen protruding outward from the cell periphery in the form of microspikes (compare Fig. 1a and b). These (PAM) often showed branching. At the same time, Cdc42Hs also caused a reduction in the number of stress fibers and an increase in diffuse and punctate actin staining. After 30 min, membrane ruffling, identified as wavy "curtains" of actin staining at the cell periphery, was also seen (Fig. 1c). By 1 h, few PAM remained but membrane ruffling was still evident. We also observed a direct relationship between the amount of Cdc42Hs injected and the extent of PAM formation (see below) and membrane ruffling. PAM and membrane ruffling were also seen when a GTPase-negative mutant, $Cdc42Hs^{G12V}$, was microinjected, suggesting that the GTP-bound form of the protein is responsible for these actin-based cytoskeletal effects (data not shown).

Specificity of Cdc42Hs effects on cell morphology. Microinjection of RhoA and Rac1 (latter shown in Fig. 1d) and K-Ras did not induce PAM formation. However, membrane ruffling was induced by the latter two proteins as described previously (6, 41). Dominant negative mutant proteins (T17N) have higher affinity for GDP than wild-type protein and prevent signalling by endogenous proteins, possibly by titrating out an activating exchange factor(s) (16, 42). Coinjection of Cdc42Hs with dominant negative $Cdc42Hs^{T17N}$ inhibited PAM formation and membrane ruffling (Fig. 1e), while coinjection of Cdc42Hs with dominant negative $Rac1^{T17N}$ inhibited only membrane ruffling (Fig. 1f). This finding suggests that Cdc42Hs directly induced PAM formation and then activated Rac1 to cause membrane ruffling. To confirm this, we coinjected Cdc42Hs with the Rac-GAP domain of *n*-chimerin (14). This resulted in loss of membrane ruffling but did not reduce the extent of PAM formation (Fig. 1g). *n*-Chimerin is predominantly a Rac-GAP with little effect on Cdc42Hs (31); its GAP domain is approximately 37-fold less potent for Cdc42Hs than for Rac1 (4). Under the conditions of the microinjection experiments, *n*-chimerin should not significantly affect the Cdc42Hs-GTP state. Rho-GDI (19) promotes the cytoplasmic localization of Rho subfamily members (RhoA, Rac1, and Cdc42Hs) and possibly prevents downstream signalling via these proteins (22, 28, 35, 46). Rho-GDI coinjected with Cdc42Hs not only inhibited the formation of Cdc42Hs-induced PAM and membrane ruffling but also reduced endogenous levels of stress fibers and polymerized actin (Fig. 1h).

Taken together, these results suggest that Cdc42Hs induces the formation of PAM, associated with a redistribution of actin polymers, followed by Rac1-mediated membrane ruffling.

Bradykinin induces changes in cell morphology similar to that seen with Cdc42Hs. As growth factors have been shown to activate Rac1 and RhoA pathways (40, 41), we screened various factors for the ability to induce PAM formation in serum-starved Swiss 3T3 cells. The bioactive peptide bradykinin was found to induce the formation of PAM and membrane ruffles with a temporal pattern similar to that observed with Cdc42Hs. PAM were formed after 10 min. There was also a reduction in stress fibers and an increase in punctate and diffuse actin staining (compare Fig. 2a and b) similar to that observed after Cdc42Hs injection. Bradykinin was found to be effective at levels down to 10 ng/ml. By 30 min after bradykinin treatment, there was a reduction in the number of PAM formed and an increase in membrane ruffling (Fig. 2c).

In contrast, PMA (200 nM), PDGF (20 ng/ml), EGF (20 ng/ml), bombesin (20 nM), insulin (2 mg/ml), and FCS (0.5%) did not induce PAM formation. As a further control, we treated cells with LPA (40 ng/ml), which is known to activate RhoA (40). LPA induced formation of stress fibers (Fig. 2d) but not of PAM. 1-Oleyl-2-acetyl-rac-glycerol, a membrane-permeable diacylglycerol, also resulted in the formation of PAM, but only at relatively high concentrations (100 μg/ml).

Since bradykinin appeared to elicit responses similar to those obtained with Cdc42Hs, the effects of the peptide were examined in relation to the proteins used to dissect the Cdc42Hs response. Microinjection of $Cdc42Hs^{T17N}$ before bradykinin treatment significantly inhibited PAM formation and the subsequent membrane ruffling (Fig. 2e). Microinjection of $Rac1^{T17N}$ or the Rac1-GAP domain of *n*-chimerin inhibited membrane ruffling but not PAM formation induced by bradykinin (Fig. 2f and g). Finally, microinjection of Rho-GDI before bradykinin treatment resulted in the reduction of all filamentous actin structures (Fig. 2h).

Together, these results suggest that the action of bradykinin is mediated by activation of Cdc42Hs which in turn activates Rac1.

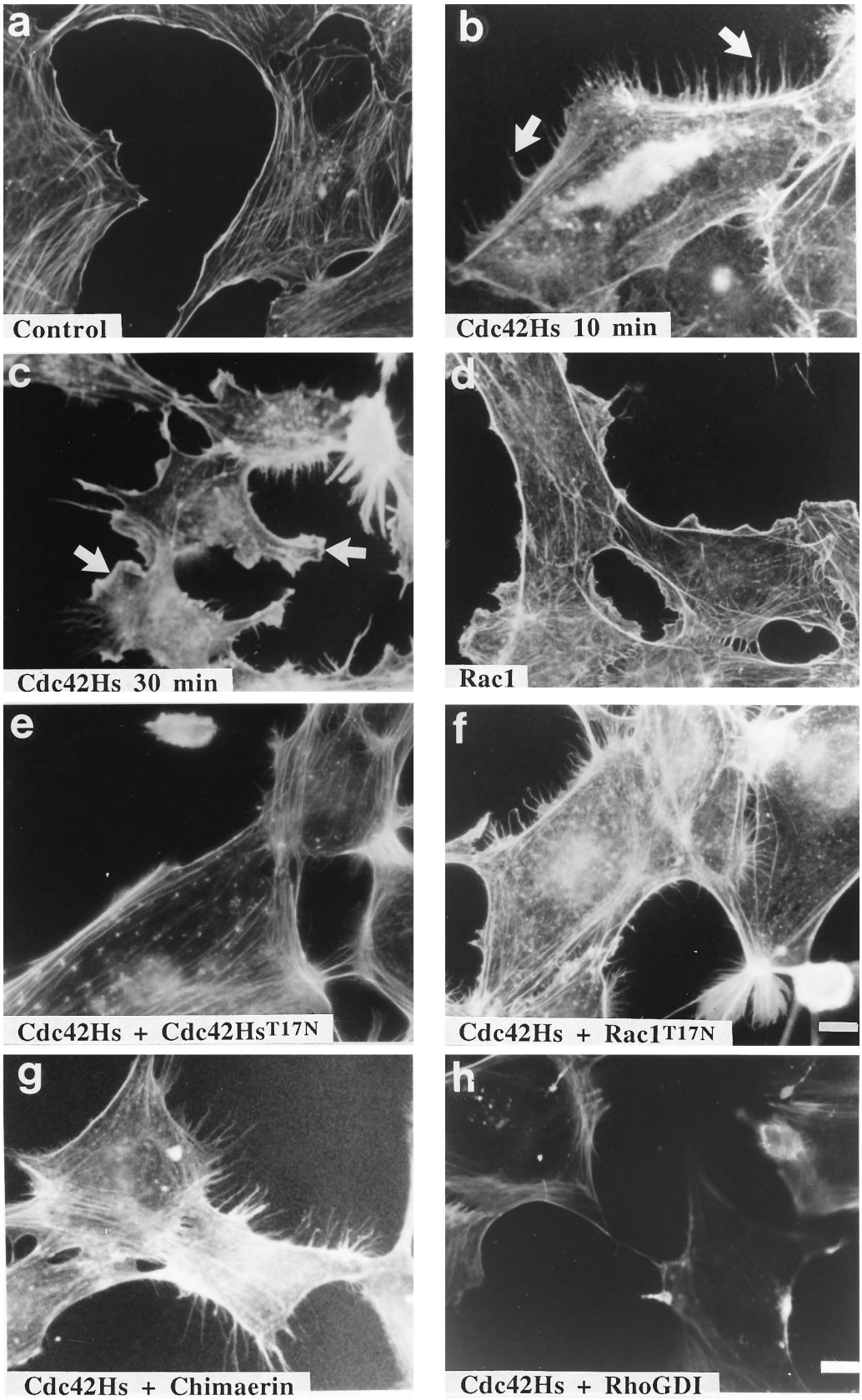

FIG. 1. Cdc42Hs promotes the formation of PAM and membrane ruffling in Swiss 3T3 fibroblasts. Proteins microinjected or coinjected were as follows: (a) none (control starved cells); (b and c) Cdc42Hs (0.5 mg/ml) for 10 min (arrows indicate PAM) and 30 min (arrows indicate areas of ruffling), respectively; (d) Rac1 (1 mg/ml) for 10 min; (e) Cdc42Hs (0.5 mg/ml) with Cdc42Hs^{T17N} (1 mg/ml) for 10 min; (f) Cdc42Hs (0.5 mg/ml) with Rac1^{T17N} (1 mg/ml) for 30 min; (g) Cdc42Hs (0.5 mg/ml) with *n*-chimerin GAP domain (0.5 mg/ml) for 10 min; (h) Cdc42Hs (0.5 mg/ml) with Rho-GDI (1 mg/ml) for 10 min. Note that panel h required 50% longer exposure than panels a to g. The bar indicates 10 μm. All cells shown in panels b to h were microinjected with the relevant protein(s).

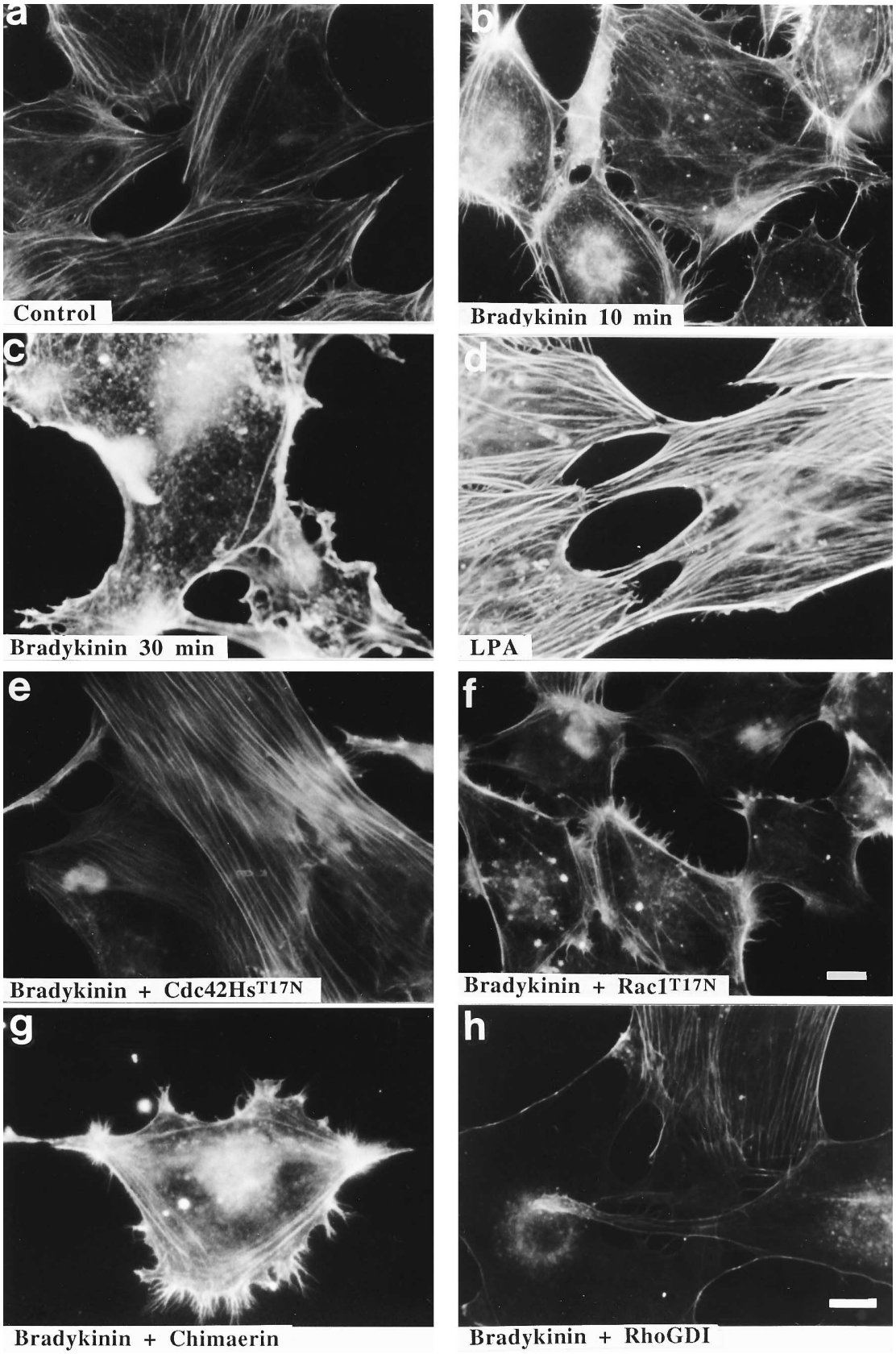

FIG. 2. Bradykinin treatment of Swiss 3T3 fibroblasts activates Cdc42Hs and Rac1 pathways. Proteins microinjected into and treatments of serum-starved fibroblasts were as follows: (a) no protein (control starved cells); (b and c) bradykinin treatment (100 ng/ml) for 10 and 30 min, respectively; (d) LPA (40 ng/ml) for 10 min; (e) Cdc42Hs^{T17N} (1 mg/ml) injection followed by bradykinin treatment; (f) Rac1^{T17N} (1 mg/ml) injection followed by bradykinin treatment; (g) injection of *n*-chimerin GAP domain (0.5 mg/ml) followed by bradykinin treatment; (h) Rho-GDI (1 mg/ml) injection followed by bradykinin treatment. Cells were incubated at 37°C for 10 min, unless otherwise stated, before fixation and staining with rhodamine-conjugated phalloidin. Note that panel h required 50% longer exposure than panels a to g. The bar indicates 10μm.

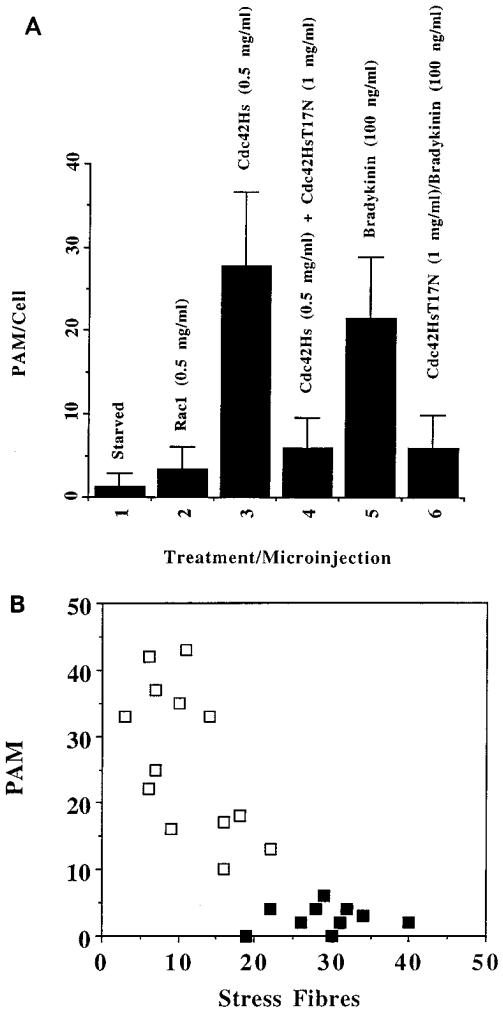

FIG. 3. Quantification of PAM and correlation of their formation with stress fiber loss. (A) Serum-starved subconfluent fibroblasts were microinjected with p21 proteins and/or treated with bradykinin and after 10 min stained with rhodamine-conjugated phalloidin. Numbers of PAM greater than 1 μm in length were estimated in randomly chosen cells. Columns: 1, control starved cells; 2, Rac1 (0.5 mg/ml) microinjected; 3, Cdc42Hs (0.5 mg/ml) microinjected; 4, Cdc42Hs (0.5 mg/ml) microinjected with $Cdc42Hs^{T17N}$ (1 mg/ml); 5, bradykinin (100 ng/ml) treatment; 6, $Cdc42Hs^{T17N}$ (1 mg/ml) microinjected followed by bradykinin (100 ng/ml) treatment. More than 50 cells were microinjected and treated, and 10 cells were photographed for quantification. Standard deviations are indicated as vertical bars. (B) Determination of numbers of PAM and stress fibers in cells microinjected with 0.5 mg of Cdc42Hs protein (white squares) or control buffer (black squares) per ml. Cells were fixed 10 min after microinjections and stained with rhodamine-conjugated phalloidin. Each square represents a single cell.

Quantitative analysis of effects of Cdc42Hs and bradykinin on actin-containing structures. To analyze the effects of Cdc42Hs microinjection and bradykinin treatment in more detail, we quantified changes in the number of PAM in populations of cells fixed 10 min after injection (Fig. 3A). It was evident that injection of Cdc42Hs but not of Rac1 led to a significant increase in the number of PAM; this number was considerably less when Cdc42Hs was coinjected with dominant negative $Cdc42Hs^{T17N}$. Bradykinin treatment was as effective as microinjection of Cdc42Hs in increasing the number of PAM; its effect was also considerably diminished by prior injection with dominant negative $Cdc42Hs^{T17N}$.

Confluent, serum-starved Swiss 3T3 cells have few stress fibers (40, 41). However, subconfluent, serum-starved cells still possessed a considerable number of stress fibers. Since subconfluent cells have fewer areas of cell-cell contact than do confluent cells, it is probable that they require more stress fibers in order to maintain substrate attachment. Interestingly, we found an inverse correlation between the number of PAM and stress fibers determined after Cdc42Hs and control microinjections (Fig. 3B). More than 50 cells were microinjected or treated in each case, and experiments were repeated at least once. Quantification was carried out on photographs of a minimum of 10 cells in each case. Addition of LPA reversed the loss of stress fibers resulting from bradykinin treatment (data not shown). In some cells injected with Cdc42Hs containing many PAM and few stress fibers, cell retraction and rounding were observed 30 min after injection, perhaps as a consequence of the loss of stress fibers.

PAM are components of both filopodia and retraction fibers. We considered that PAM were likely to be components of dynamic peripheral cellular structures that were undergoing either protrusion or retraction prior to fixation and staining with phalloidin. To investigate the relationship of PAM to these structures, cells were treated with bradykinin and changes in their morphology were monitored by time-lapse phase-contrast microscopy prior to staining. Figure 4 shows the analysis of one such cell. More peripheral structures were revealed by phalloidin staining than by phase-contrast microscopy, reflecting differences in sensitivity of detection. Over a 10-min period after exposure to bradykinin, protrusions of up to 12 μm were seen to form (compare Fig. 4a and b). We designated these protrusions as filopodia because of their similarity in morphology, size, and kinetic nature to those previously described (5, 8). PAM, detected by phalloidin staining, were indeed found to be components of these filopodia (Fig. 4d). However PAM also contributed to fibrous structures at regions where there was cell retraction; these probably represented retraction fibers (12). It is clear that filopodia and retraction fibers are indistinguishable on the basis of phalloidin staining (Fig. 4d), and time-lapse analysis is essential to observe their formation.

Cdc42Hs promotes the formation of filopodia. To investigate the effect of Cdc42Hs on filopodium formation, cells were microinjected with the protein and changes in their morphology were analyzed by time-lapse microscopy. At least 10 cells were individually monitored, and experiments were repeated on two or more occasions for all phase-contrast analyses. Within a few minutes of microinjection of Cdc42Hs, filopodia could be seen protruding from the cell (Fig. 5A; compare panels a and b). These filopodia normally extended in length from 1 to 15 μm. Over the next 10 min, new filopodia were formed while some existing filopodia decreased in size (Fig. 5A, panel c). Occasionally the cell surface was seen to extend between the filopodia to form lamellipodia (filled-in area in Fig. 5A, panel d). Subsequent to filopodium formation, most cells microinjected with Cdc42Hs displayed retraction as well as membrane ruffles and lamellipodia (Fig. 1). Membrane ruffles were identified by phase-contrast microscopy as the formation of transient darkened cell edges or surfaces, and lamellipodia were identified as cell surface expansions. Serum-starved control or bovine serum albumin (BSA)-microinjected cells showed very little change in morphology over a 15-min time course (Fig. 5B, panels c and d). Microinjection with purified RhoA, Rac1, or K-Ras proteins did not induce filopodia (data not shown).

In cells not possessing filopodia, microinjection with the dominant negative $Cdc42Hs^{T17N}$ had no effect on cell morphology (Fig. 5B, panels a and b). However, cells with existing

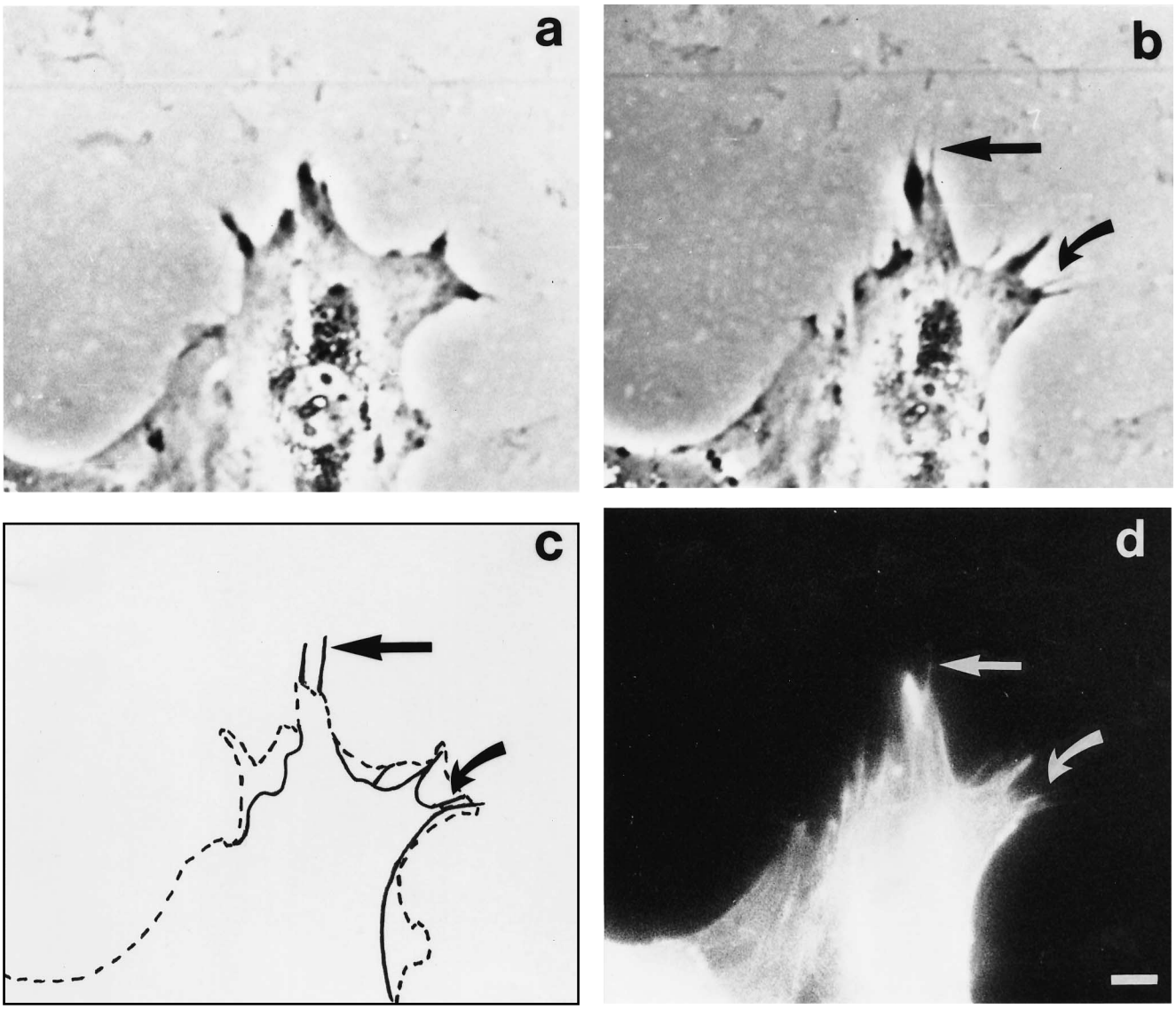

FIG. 4. PAM are components of filopodia and retraction fibers in Swiss 3T3 fibroblasts. A serum-starved subconfluent fibroblast was treated with 100 ng of bradykinin per ml and photographed at 0 (a) min and 10 (b) min. (c) Diagrammatic representation indicating cell shape at 0 min (dashed line) and changes in shape after 10 min (bold lines). (d) The cell was then fixed and stained with rhodamine-phalloidin to stain filamentous actin. Note an example of a filopodium protruding from the cell (straight arrows) and an example of a retraction fiber resulting from a region of cell retraction (curved arrows). The bar indicates 7 μm.

filopodia when microinjected with $Cdc42Hs^{T17N}$ displayed a rapid loss of filopodia (in 10 cells examined, approximately 75% of filopodia were lost within 4 min). This finding suggests that Cdc42Hs activity may be necessary for the maintenance of filopodia. When cells were microinjected with dominant negative $Rac1^{T17N}$, existing filopodia were not lost (data not shown). Dominant negative $Cdc42Hs^{T17N}$ appears to act specifically on the Cdc42Hs pathway because it did not inhibit membrane ruffling induced by Rac1, nor did it affect levels of stress fibers. Specificity of response was also observed following use of two other point mutations of Cdc42Hs. Microinjection of the mutant $Cdc42Hs^{D38A}$ did not result in significant filopodium formation, while microinjection of the mutant $Cdc42Hs^{Q61L}$ resulted in filopodium formation to a level at least as high as that seen following microinjection of $Cdc42Hs^{G12V}$ (data not shown). These results are consistent with the report that the corresponding Rac2 mutant $Rac2^{Q61L}$ was more effective than wild-type Rac2 in inducing ruffles whereas $Rac2^{D38A}$ was ineffective (51). The equivalent D38A mutation in Ras leads to a loss of effector function, while the $Cdc42Hs^{Q61L}$ mutation, like Ras^{Q61L}, results in the protein having negligible GTPase activity (see Materials and Methods).

Bradykinin also promotes filopodium formation. When analyzed over the same time course, bradykinin was found to promote the formation of filopodia similar to that observed upon Cdc42Hs microinjection (Fig. 6). Areas of cell expansion and cell retraction were also seen (shown diagrammatically in Fig. 6d). As with Cdc42Hs microinjection, most cell retraction occurred after the period of maximal filopodium formation. Bradykinin was effective at promoting filopodium formation at levels down to 10 ng/ml.

Bradykinin-promoted filopodium formation is mediated by Cdc42Hs. Using time-lapse analysis, we quantified the forma-

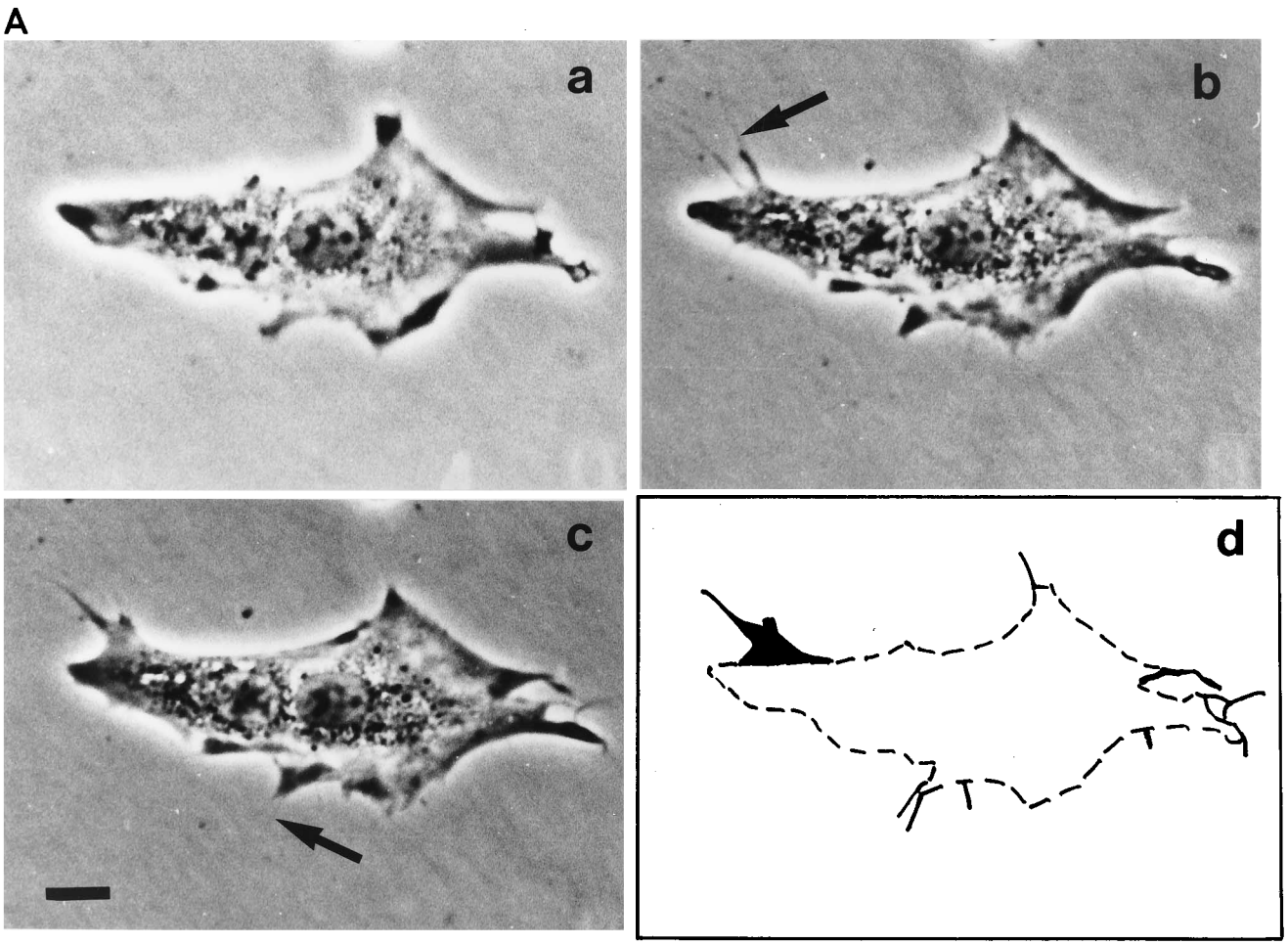

FIG. 5. Cdc42Hs promotes the formation of filopodia in Swiss 3T3 fibroblasts. (A) Cdc42Hs protein (0.5 mg/ml) was microinjected into serum-starved subconfluent fibroblasts, which were photographed under phase-contrast microscopy at 0 (a), 5 (b), and 15 (c) min after microinjection. Arrows (b and c) indicate filopodia which have formed. (d) Diagrammatic representation showing cell shape at 0 min (dashed lines), new filopodia present at 15 min (black lines extending out from cell), and areas of cell extension as lamellipodia (filled-in areas). Some cells also showed areas of retraction. The bar indicates 10 μm. (B) Dominant negative $Cdc42Hs^{T17N}$ protein (1 mg/ml) was microinjected into two serum-starved subconfluent fibroblasts and photographed at 0 (a) and 15 (b) min after microinjection. Control BSA (0.5 mg/ml) was microinjected into the cell in the center of the field, which was then photographed at 0 (c) and 15 (d) min. The bar indicates 10 μm.

tion of new filopodia during the first 15 min following treatment with bradykinin or microinjection with Cdc42Hs and its mutants (Fig. 7). Filopodium formation, which was negligible in control starved cells (lane 1), was considerably increased upon treatment with 10% foetal calf serum (FCS, lane 2). The extent of filopodium formation promoted by bradykinin treatment (columns 3 to 5) and microinjection of Cdc42Hs (columns 6 to 8) appeared to be concentration dependent. The GTPase-deficient mutant $Cdc42Hs^{G12V}$ (column 9) was as effective as wild-type Cdc42Hs. The effect of bradykinin was inhibited by prior microinjection of the dominant inhibitory mutant $Cdc42Hs^{T17N}$ (column 10) but not of the Rac1 counterpart $Rac1^{T17N}$ (column 11). As previously mentioned, microinjection of the mutant $Cdc42Hs^{T17N}$ did not promote filopodium formation (column 12). Coinjection of this mutant and the wild type was also without effect (data not shown).

These results show that the extent of filopodium formation was dependent on the concentration of the causative agent and that the effects of bradykinin were mediated by Cdc42Hs. Treatment with EGF at 100 ng/ml (but not at 10 ng/ml) also resulted in significant production of filopodia, but it was not as potent as bradykinin (data not shown). In contrast, treatment with PMA (200 nM), PDGF (100 ng/ml), or LPA (40 ng/ml) did not result in filopodium formation.

The effects of bradykinin treatment in relation to Cdc42Hs activity on the formation of lamellipodia and ruffles and on cell retraction subsequent to filopodium formation were also examined. The results are summarized in Table 1. Microinjection of the dominant negative $Cdc42Hs^{T17N}$ was able to prevent these effects of bradykinin, while microinjection of dominant negative $Rac1^{T17N}$ prevented only the formation of lamellipodia and ruffles. FCS (10%) also resulted in lamellipodia and ruffles and in cellular retraction. In contrast, microinjection with Rac1 or treatment with PDGF did not result in significant retraction, although lamellipodia and membrane ruffles were observed.

DISCUSSION

Members of the subfamily of Rho proteins have been ascribed roles in the formation of particular actin microfilament structures. Rac1 is involved in the formation of cortical actin as part of membrane ruffling (41), while RhoA causes the formation of stress fibers (39, 40). Here we show that Cdc42Hs,

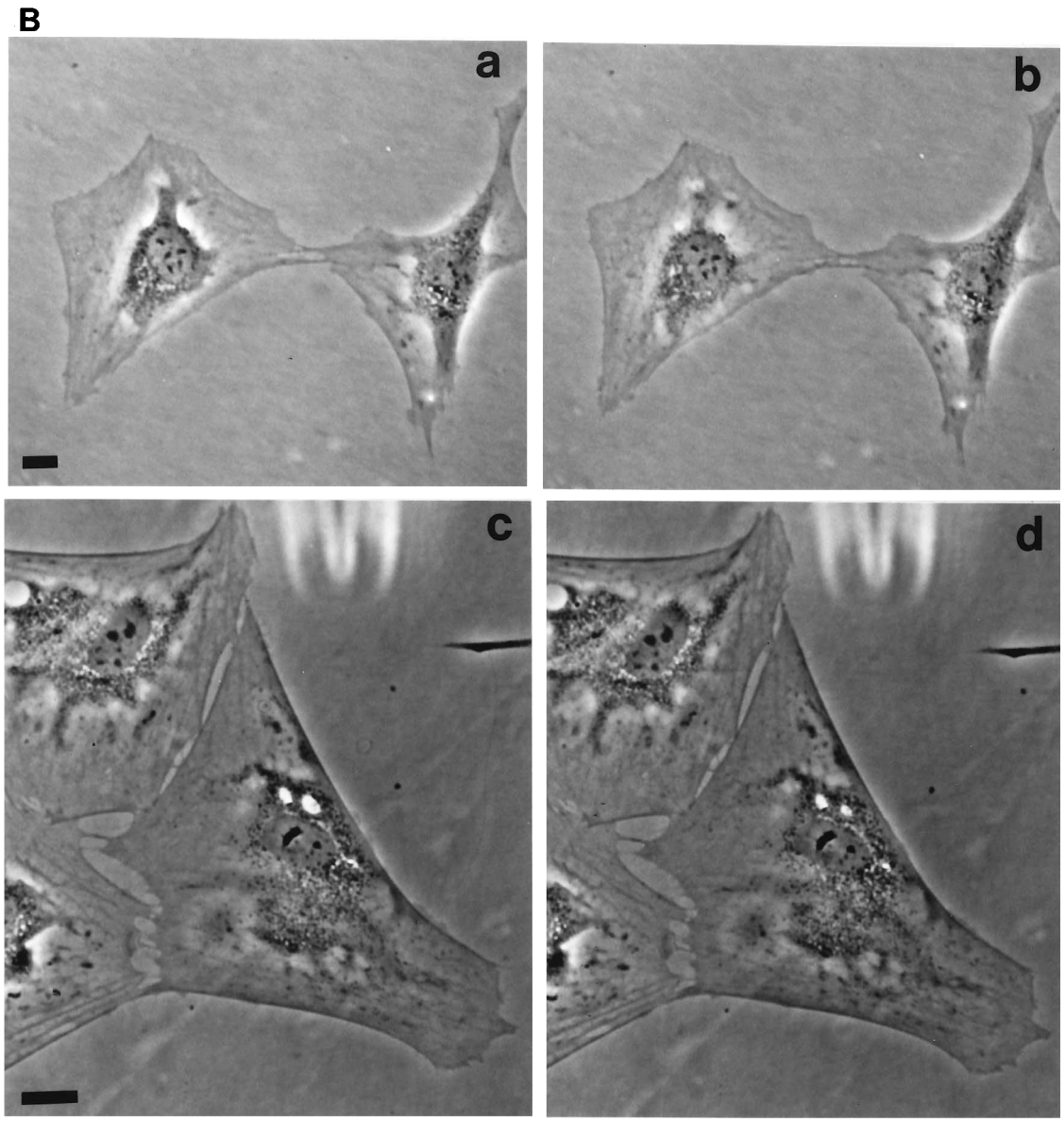

FIG. 5—*Continued.*

another family member, is involved in the formation of actin-containing microspikes at the periphery of the cell. Some of these PAM are components of filopodia which protrude out from the cortex of the cell. Cdc42Hs microinjection also results in a reduction in stress fibers and an increase in diffuse and punctate actin staining. This redistribution of actin polymers could be due to PAM and stress fibers being generated from a common pool of actin. Another possibility is that both structures require the same actin-binding protein or proteins for polymerization. It is interesting that fibroblasts overexpressing the intestinal actin-binding protein villin produce numerous actin-containing microvilli with a concomitant loss of stress fibers (18). We found that bradykinin but not PDGF, insulin, PMA, LPA, or bombesin treatment of cells resulted in morphological and cytoskeletal effects similar to that seen upon Cdc42Hs microinjection. Bradykinin is a mediator of inflammation and hypotension and is a mitogen, thought to act through bradykinin receptor-linked G proteins, which leads to activation of phospholipases C and D and release of internal calcium (9, 48, 50). Bombesin and LPA are, like bradykinin, thought to act through receptors linked to G proteins (7, 49) but cause different morphological and cytoskeletal effects. In contrast, PDGF, EGF, and insulin operate through receptor tyrosine kinases (13). Together, these findings suggest that Rho subfamily members and Ras coordinate cellular changes resulting from the activation of a variety of cell surface receptors.

Microinjection of Ras and Rho subfamily proteins into mammalian cells has revealed a hierarchy of interactions. Ras can activate Rac1, and Rac1 can activate RhoA (41). Our study incorporates Cdc42Hs into this hierarchy by showing it to activate Rac1 (Fig. 8). Membrane ruffling and lamellipodium formation can be induced through microinjection of either Rac1 or Cdc42Hs, in the latter case following the formation of filopodia. This hierarchy is also reflected in the action of various growth factors with, for instance, PDGF inducing mem-

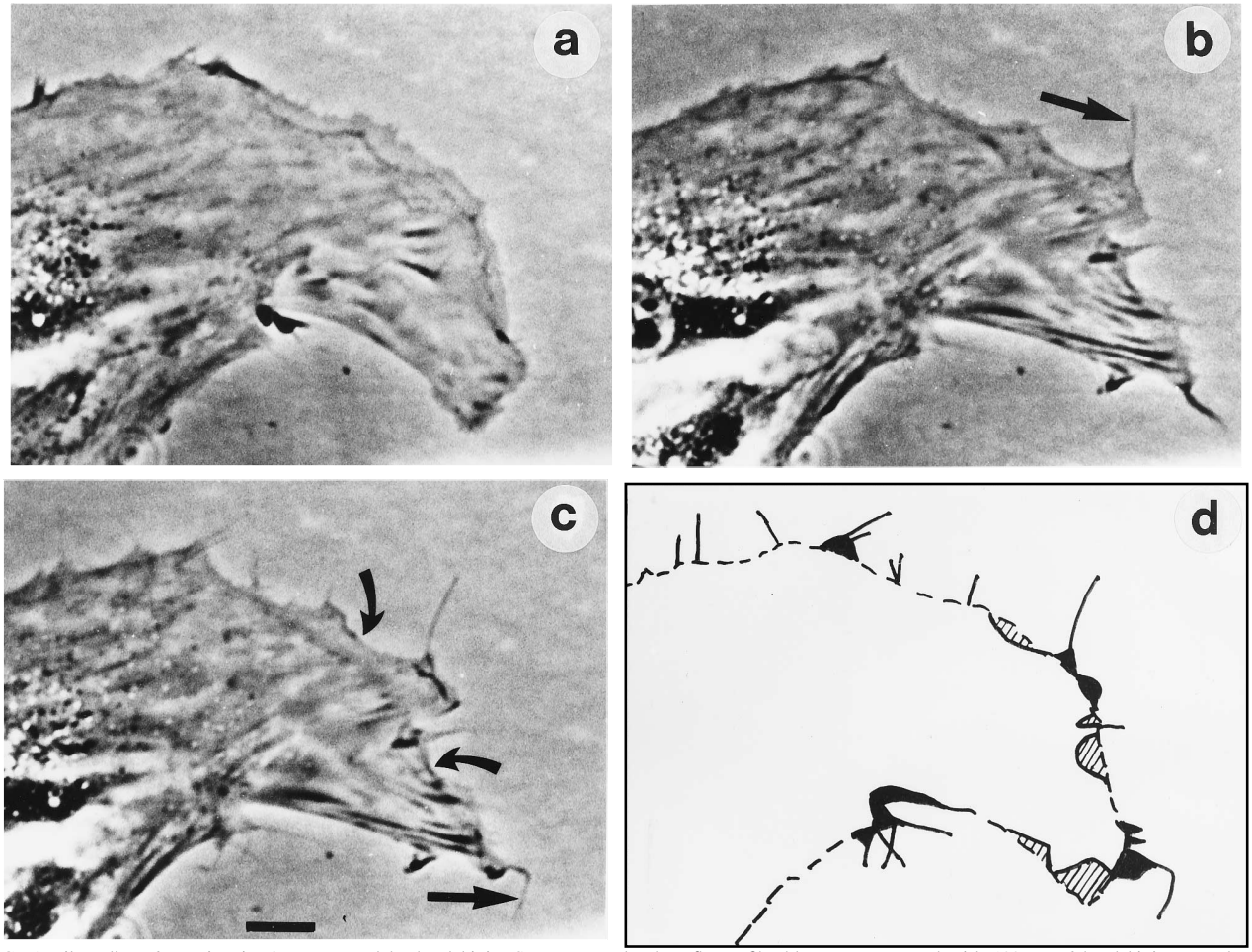

FIG. 6. Filopodium formation is also promoted by bradykinin. Serum-starved subconfluent fibroblasts were treated with 100 ng of bradykinin per ml and photographed under phase-contrast microscopy after 0 (a), 5 (b), and 15 (c) min. Straight arrows (b and c) indicate filopodium extensions; curved arrows (c) indicate areas of cell retraction. (d) Diagrammatic representation of the cell indicating original cell shape at 0 min (dashed lines), filopodia present at 15 min (black extension lines), areas of cell extension as lamellipodia at 15 min (filled-in areas), and areas of cell retraction at 15 min (hatched areas). The bar indicates 5 μm.

brane ruffling directly (via Rac1) without affecting filopodium formation, while bradykinin induces membrane ruffling (again via Rac1) subsequent to filopodium formation (via Cdc42Hs) (Table 1). In addition, Cdc42Hs may inhibit RhoA signalling because PAM formation is associated with a loss of stress fibers (Fig. 8). The mechanisms for the cross talk between members of the Rho family p21 proteins are unclear at present. However, proteins which are potentially GDP/GTP exchange factors and GAPs, such as Bcr and Abr (25, 47), which can act on more than one type of p21 may represent one means by which cross talk could occur. Interactions between different p21 signalling pathways may allow coordinated and sequential cytoskeletal modifications important for events such as cell migration, mitosis, or neural growth cone movement (24, 30, 37).

Filopodia are processes which form at the cell periphery and protrude outward. They are believed to play a role in initiating changes in cell shape and migration. They are thought to have an important function as sensory structures to monitor the environment and direct polarized growth, both in fibroblasts (5) and in neural growth cones (26). For instance, stimulation of a single filopodium can result in reorientation of the whole growth cone (38), while growth cones lacking filopodia are no longer able to navigate (11). Furthermore, actin polymeriza-

TABLE 1. Determination of morphological changes (excluding filopodium formation) observed by phase-contrast time-lapse microscopy within 20 min of p21 protein microinjections or treatment with various factors[a]

Treatment or microinjection	Formation of lamellipodia[b] and membrane ruffles[c]	Retraction
Control (starved)	−	−
Rac1 (0.5 mg/ml)	++	−
Cdc42Hs (0.5 mg/ml)	+	+
$Cdc42Hs^{T17N}$ (1 mg/ml)	−	−
Bradykinin (10 ng/ml)	+	+
Bradykinin (100 ng/ml) + $Cdc42Hs^{T17N}$ (1 mg/ml)	−	−
Bradykinin (100 ng/ml) + $Rac1^{T17N}$ (1 mg/ml)	−	+
PDGF (10 ng/ml)	++	−
LPA (20 ng/ml)	−	−
FCS (10%)	++	+

[a] At least 10 serum-starved subconfluent cells picked randomly were monitored in each case. −, no significant activity; +, low activity (estimated to affect less than 50% of the cell surface); ++, high activity (estimated to affect more than 50% of the cell surface).
[b] Expansions from the cell edge.
[c] Formation of transient darkened cell edges or surfaces.

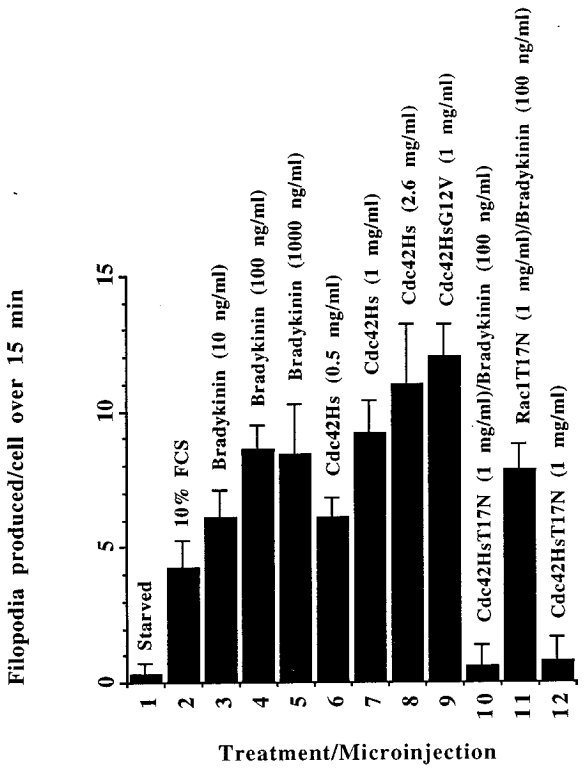

FIG. 7. Bradykinin-promoted formation of filopodia is mediated by Cdc42Hs. Randomly chosen serum-starved subconfluent fibroblasts were monitored by time-lapse phase-contrast microscopy for 15-min durations following microinjection and treatment, and the formation of new filopodia was quantified. At least 10 cells were monitored for each microinjection and treatment, and experiments were repeated two to four times. Columns: 1, starved control cells; 2, 10% FCS; 3, bradykinin (10 ng/ml); 4, bradykinin (100 ng/ml); 5, bradykinin (1 μg/ml); 6, microinjection with Cdc42Hs (0.5 mg/ml); 7, Cdc42Hs (1 mg/ml); 8, Cdc42Hs (2.6 mg/ml); 9, $Cdc42Hs^{G12V}$ (1 mg/ml); 10, dominant negative $Cdc42Hs^{T17N}$ (1 mg/ml) followed by treatment with bradykinin (100 ng/ml); 11, dominant negative $Rac1^{T17N}$ (1 mg/ml) followed by treatment with bradykinin (100 ng/ml); 12, dominant negative $Cdc42Hs^{T17N}$ (1 mg/ml). Standard deviations are shown as vertical bars.

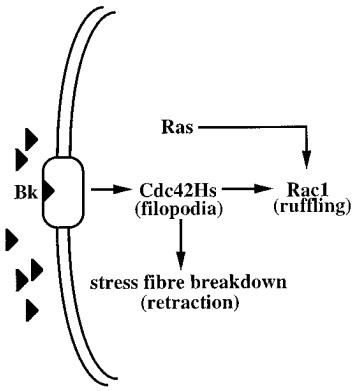

FIG. 8. Signalling pathway for Cdc42Hs effects on fibroblast cell morphology. Double lines indicate plasma membrane, and the box indicates bradykinin receptor. Activation of the Cdc42Hs pathway, either by bradykinin (Bk) or microinjection of cells, results in the production of filopodia. Following this initial morphological change, there is a reduction of stress fibers and Rac1-mediated membrane ruffling and lamellipodium formation. Ras does not appear to activate Cdc42Hs but can cause Rac1-mediated membrane ruffling. Finally, it is possible that the Cdc42Hs-mediated reduction in stress fibers results from an inhibition of RhoA signalling.

tion and depolymerization appear to be of fundamental importance for the formation and retraction of filopodia (37, 45). Recently, filopodia and membrane ruffling have been shown to be involved in the passive uptake of *Salmonella typhimurium* (17). All of these processes involve remodelling of the cell surface, and in particular, the filopodia produced during neural growth cone extension (8) are similar in structure and kinetic nature to those of fibroblasts produced upon Cdc42Hs microinjection or bradykinin treatment. Thus, it would be interesting to test directly for the possible involvement of Cdc42Hs in neural growth cone development and migration. In conclusion, our results show that Cdc42Hs promotes filopodium formation and a redistribution of actin polymers and that Cdc42Hs and Rac1 may act sequentially in promoting the formation of actin-containing structures important for determining cell morphology and polarity.

ACKNOWLEDGMENTS

We thank Tom Leung for RhoA and Cdc42Hs cDNAs and Peter Lowe for K-Ras protein.

We thank the Singapore-Glaxo Research Fund for financial support.

REFERENCES

1. **Abo, A., E. Pick, A. Hall, N. Totty, C. G. Teahan, and A. W. Segal.** 1991. Activation of the NADPH oxidase involves the small GTP-binding protein p21Rac1. Nature (London) **353:**668–670.
2. **Adams, A. E. M., D. I. Johnson, R. M. Longnecker, B. F. Sloat, and J. R. Pringle.** 1990. CDC42 and CDC43, two additional genes involved in budding and the establishment of cell polarity in the yeast *Saccharomyces cerevisiae*. J. Cell Biol. **111:**131–142.
3. **Ahmed, S., J. Lee, R. Kozma, A. Best, C. Monfries, and L. Lim.** 1993. A novel functional target for tumour-promoting phorbol esters and lysophosphatidic acid. The racGTPase activating protein n-chimaerin. J. Biol. Chem. **268:** 10709–10712.
4. **Ahmed, S., J. Lee, L.-P. Wen, Z. Zhao, J. Ho, A. Best, R. Kozma, and L. Lim.** 1994. Breakpoint cluster region gene product-related domain of n-chimaerin. Discrimination between Rac-binding and GTPase activating residues by mutational analysis. J. Biol. Chem. **269:**17642–17648.
5. **Albrecht-Buehler, G.** 1976. Filopodia of spreading 3T3 cells. J. Cell Biol. **69:**275–286.
6. **Bar-Sagi, D., and J. R. Feramsico.** 1986. Induction of membrane ruffling and fluid-phase pinocytosis in quiescent fibroblasts by ras protein. Science **233:** 1061–1068.
7. **Battey, J. F., J. M. Way, M. H. Corjay, H. Shapira, K. Kusano, R. Harkins, J. M. Wu, T. Slattery, E. Mann, and R. I. Feldman.** 1991. Molecular cloning of the bombesin/gastrin-releasing peptide receptor from Swiss 3T3 cells. Proc. Natl. Acad. Sci. USA **88:**395–399.
8. **Bray, D., and K. Chapman.** 1985. Analysis of microspike movements on the neuronal growth cone. J. Neurosci. **5:**3204–3213.
9. **Burch, R. M., and D. J. Kyle.** 1992. Recent developments in the understanding of bradykinin receptors. Life Sci. **50:**829–838.
10. **Chardin, P., P. Boquet, P. Madaule, M. R. Popoff, E. J. Rubin, and D. M. Gill.** 1989. The mammalian G protein RhoC is ADP-ribosylated by *Clostridium botulinum* exoenzyme C3 and affects actin microfilament in Vero cells. EMBO J. **8:**1087–1092.
11. **Chien, C.-B., D. E. Rosenthal, W. A. Harris, and C. E. Holt.** 1993. Navigational errors made by growth cones without filopodia in the embryonic *Xenopus* brain. Neuron **11:**237–251.
12. **Cramer, L., and T. J. Mitchison.** 1993. Moving and stationary actin-filaments are involved in spreading of post-mitotic PTK2 cells. J. Cell Biol. **122:**833–843.
13. **Cross, M., and T. M. Dexter.** 1991. Growth factors in development, transformation, and tumorigenesis. Cell **64:**271–280.
14. **Diekmann, D., S. Brill, M. D. Garrett, N. Totty, J. Hsuan, C. Monfries, C. Hall, L. Lim, and A. Hall.** 1991. Bcr encodes a GTPase-activating protein for p21rac. Nature (London) **351:**400–402.
15. **Drubin, D. G.** 1991. Development of cell polarity in budding yeast. Cell **65:**1093–1096.
16. **Farnsworth, C. L., and L. Feig.** 1991. Dominant inhibitory mutations in the Mg^{2+}-binding site of H-Ras prevent its activation by GTP. Mol. Cell. Biol. **11:**4822–4829.
17. **Francis, C. L., T. A. Ryan, B. D. Jones, S. J. Smith, and S. Falkow.** 1993. Ruffles induced by *Salmonella* and other stimuli direct macropinocytosis of bacteria. Nature (London) **364:**639–642.
18. **Friederich, E., C. Huet, M. Arpin, and D. Louvard.** 1989. Villin induces

microvilli growth and actin redistribution in transfected fibroblasts. Cell **59:**461–475.
19. **Fukumoto, Y., K. Kaibuchi, Y. Hori, H. Fujioka, S. Araki, T. Ueda, A. Kikuchi, and Y. Takai.** 1990. Molecular cloning and characterisation of a novel type of regulatory protein (GDI) for the rho proteins, ras p21-like small GTP-binding proteins. Oncogene **5:**1321–1328.
20. **Guan, K., and J. E. Dixon.** 1991. Eukaryotic proteins expressed in *Escherichia coli*: an improved thrombin cleavage and purification procedure of fusion proteins with glutathione S-transferase. Anal. Biochem. **192:**262–267.
21. **Hall, A.** 1992. Ras-related GTPases and the cytoskeleton. Mol. Biol. Cell **3:**475–479.
22. **Hancock, J. F., and A. Hall.** 1993. A novel role for Rho-GDI as an inhibitor of GAP proteins. EMBO J. **12:**1915–1921.
23. **Hart, M. J., A. Eva, T. Evans, S. A. Aaronson, and R. Cerione.** 1991. Catalysis of guanine nucleotide exchange on the CDC42Hs protein by the dbl oncogene product. Nature (London) **354:**311–314.
24. **Heidemann, S. R., and R. E. Buxbaum.** 1991. Growth cone motility. Curr. Opin. Neurobiol. **1:**339–345.
25. **Heisterkamp N., V. Kaartinen, S. van Soest, G. M. Bokoch, and J. Groffen.** 1993. Human abr encodes a protein with GAP rac activity and homology to the dbl nucleotide exchange factor domain. J. Biol. Chem. **268:**16903–16906.
26. **Hynes, R. O., and A. D. Lander.** 1992. Contact and adhesive specificities in the associations, migrations, and targeting of cells and axons. Cell **68:**303–322.
27. **Johnson, D. I., and J. R. Pringle.** 1990. Molecular characterisation of CDC42, a *Saccharomyces cerevisiae* gene involved in the developmental of cell polarity. J. Cell Biol. **111:**143–152.
28. **Kishi, K., T. Sasaki, S. Kuroda, T. Itoh, and Y. Takai.** 1993. Regulation of cytoplasmic division of *Xenopus* embryo by rho and its inhibitory GDP/GTP exchange protein (rhoGDI). J. Cell Biol. **120:**1187–1195.
29. **Knaus, U. G., P. J. Heyworth, T. Evans, J. T. Curnutte, and G. M. Bokoch.** 1991. Regulation of phagocyte oxygen radical production by the GTP-binding protein Rac2. Science **254:**1512–1515.
30. **Lee, J., A. Ishihara, and K. Jacobson.** 1993. How do cells move along surfaces? Trends Cell Biol. **3:**366–370.
31. **Manser, E., T. Leung, C. Monfries, M. Teo, C. Hall, and L. Lim.** 1992. Diversity and versatility of GTPase activating proteins for the p21 Rho subfamily of Ras G proteins detected by a novel overlay assay. J. Biol. Chem. **267:**16025–16028.
32. **Manser, E., T. Leung, H. Salihuddin, L. Tan, and L. Lim.** 1993. A non-receptor tyrosine kinase that inhibits the GTPase activity of $p21^{cdc42}$. Nature (London) **363:**364–367.
33. **Manser, E., T. Leung, H. Salihuddin, Z.-S. Zhao, and L. Lim.** 1994. A brain serine/threonine kinase activated by Cdc42 and Rac1. Nature (London) **367:**40–46.
34. **McCormick, F.** 1989. *ras* GTPase activating protein: signal transmitter and signal terminator. Cell **56:**5–8.
35. **Muira, Y., A. Kikuchi, T. Musha, S. Kuroda, H. Yaku, T. Sasaki, and Y. Takai.** 1993. Regulation of morphology by rho p21 and its inhibitory GDP/GTP exchange protein (rho GDI) in Swiss 3T3 cells. J. Biol. Chem. **268:**510–515.
36. **Munemitsu, S., M. A. Innis, R. Clark, F. McCormick, A. Ullrich, and P. Polakis.** 1990. Molecular cloning and expression of a G25K cDNA, the human homolog of the yeast cell cycle gene *CDC42*. Mol. Cell. Biol. **10:**5977–5982.
37. **O'Connor, T. P., and D. Bentley.** 1993. Accumulation of actin subsets of pioneer growth cone filopodia in response to neural and epithelial guidance cues *in situ*. J. Cell Biol. **123:**935–948.
38. **O'Connor, T. P., J. S. Duerr, and D. Bentley.** 1990. Pioneer growth cone steering decisions mediated by single filopodial contacts *in situ*. J. Neurosci. **10:**3935–3946.
39. **Paterson, H. F., A. J. Self, M. D. Garratt, I. Just, K. Aktories, and A. Hall.** 1990. Microinjection of recombinant p21Rho induces rapid changes in cell morphology. J. Cell Biol. **111:**1001–1007.
40. **Ridley, A. J., and A. Hall.** 1992. The small GTP-binding protein rho regulates the assembly of focal adhesions and actin stress fibres in response to growth factors. Cell **70:**389–399.
41. **Ridley, A. J., H. F. Paterson, C. L. Johnstone, D. Diekmann, and A. Hall.** 1992. The small GTP-binding protein rac regulates growth factor-induced membrane ruffling. Cell **70:**401–410.
42. **Schweighoffer, F., H. Cai, M. C. Checallier-Multon, I. Fath, G. Cooper, and B. Tocque.** 1993. The *Saccharomyces cerevisiae* SDC25 C-domain gene product overcomes the dominant inhibitory activity of Ha-Ras Asn-17. Mol. Cell. Biol. **13:**39–43.
43. **Shinjo, K., J. G. Koland, M. J. Hart, V. Narasimhan, D. I. Johnson, T. Evans, and R. Cerione.** 1990. Molecular cloning of the gene for the human placental GTP-binding protein Gp (G25K): identification of this GTP-binding protein as the human homolog of the yeast cell-division-cycle protein CDC42. Proc. Natl. Acad. Sci. USA **87:**9853–9857.
44. **Smith, D. B., and K. S. Johnson.** 1988. Single-step purification of polypeptides expressed in *Escherichia coli* as fusions with glutathione S-transferase. Gene **67:**31–40.
45. **Smith, S. J.** 1988. Neuronal cytomechanics: the actin-based motility of growth cones. Science **242:**708–714.
46. **Takaishi, K., A. Kikuchi, K. Kuroda, K. Kotani, T. Sasaki, and Y. Takai.** 1993. Involvement of *rho* p21 and its inhibitory GDP/GTP exchange protein (*rho* GDI) in cell motility. Mol. Cell. Biol. **13:**72–79.
47. **Tan, E.-C., T. Leung, E. Manser, and L. Lim.** 1993. The human active breakpoint cluster region related gene encodes a brain protein with homology to guanine nucleotide exchange proteins and GTPase activating proteins. J. Biol. Chem. **268:**26409–26415.
48. **van Blitterswijk, W. J., H. Hilkmann, J. de Widt, and R. L. van der Bend.** 1991. Phospholipid metabolism in bradykinin-stimulated human fibroblasts. II. Phosphatidylcholine breakdown by phospholipases C and D: involvement of protein kinase C. J. Biol. Chem. **266:**10344–10350.
49. **van Corven, E. J., A. Groenink, K. Jalink, T. Eichholtz, and W. H. Moolenaar.** 1989. Lysophosphatidate-induced cell proliferation: identification and dissection of signalling pathways mediated by G proteins. Cell **59:**45–54.
50. **Wheeler, L. A., D. D. Goodrum, and G. Sachs.** 1990. Role of protein kinase C in the regulation of cytosolic Ca^{++} in A431 cells: separation of growth factor and bradykinin pathways. J. Membr. Biol. **118:**77–91.
51. **Xu, X., D. C. Barry, J. Settleman, M. A. Schwartz, and G. M. Bokoch.** 1994. Different structural requirements for GTPase-activating protein responsiveness and NADPH oxidase activation by Rac. J. Biol. Chem. **269:**23569–23574.